SUBMITTED TO THE ASTROPHYSICAL JOURNAL LETTERS. PLEASE DO NOT REDISTRIBUTE.
Preprint typeset using LaTeX style emulateapj v. 08/22/09

THE PRIMEVAL POPULATIONS OF THE ULTRA-FAINT DWARF GALAXIES[1]

THOMAS M. BROWN[2], JASON TUMLINSON[2], MARLA GEHA[3], EVAN N. KIRBY[4,5], DON A. VANDENBERG[6], RICARDO R. MUÑOZ[7], JASON S. KALIRAI[2], JOSHUA D. SIMON[8], ROBERTO J. AVILA[2], PURAGRA GUHATHAKURTA[9], ALVIO RENZINI[10], HENRY C. FERGUSON[2]

Submitted to The Astrophysical Journal Letters. Please do not redistribute.

ABSTRACT

We present new constraints on the star formation histories of the ultra-faint dwarf (UFD) galaxies, using deep photometry obtained with the *Hubble Space Telescope (HST)*. A galaxy class recently discovered in the Sloan Digital Sky Survey, the UFDs appear to be an extension of the classical dwarf spheroidals to low luminosities, offering a new front in efforts to understand the missing satellite problem. They are the least luminous, most dark-matter dominated, and least chemically-evolved galaxies known. Our *HST* survey of six UFDs seeks to determine if these galaxies are true fossils from the early universe. We present here the preliminary analysis of three UFD galaxies: Hercules, Leo IV, and Ursa Major I. Classical dwarf spheroidals of the Local Group exhibit extended star formation histories, but these three Milky Way satellites are at least as old as the ancient globular cluster M92, with no evidence for intermediate-age populations. Their ages also appear to be synchronized to within $\sim$1 Gyr of each other, as might be expected if their star formation was truncated by a global event, such as reionization.

Subject headings: Local Group — galaxies: dwarf — galaxies: photometry — galaxies: evolution — galaxies: formation — galaxies: stellar content

1. INTRODUCTION

Although the Lambda Cold Dark Matter paradigm is consistent with many observable phenomena, such as the growth of large scale structure, discrepancies arise at small scales. One of the most prominent issues is that it predicts many more dark-matter halos than are actually seen as dwarf galaxies (e.g., Moore et al. 1999). A possible solution has arisen with the recent discovery of additional satellites around the Milky Way (e.g., Willman et al. 2005; Zucker et al. 2006; Belokurov et al. 2007) and Andromeda (e.g., Zucker et al. 2007) in the Sloan Digital Sky Survey (York et al. 2000) and other wide-field surveys (e.g., McConnachie et al. 2009).

The newly-discovered ultra-faint dwarf (UFD) galaxies appear to be an extension of the classical dwarf spheroidals (dSphs) to lower luminosities ($M_V \gtrsim -8$ mag). UFD luminosities are comparable to those of globular clusters, but one distinction in the former is the presence of dark matter. Even the most massive globular clusters have mass-to-light ratios (M/L_V) of $\sim$2 (e.g., Baumgardt et al. 2009; van de Ven et al. 2006), precluding significant dark matter. In contrast, all known dwarf galaxies have higher M/L_V (Kalirai et al. 2010 and references therein). UFD kinematics are clearly dark matter-dominated, with $M/L_V > 100$ (e.g., Kleyna et al. 2005; Simon & Geha 2007; Muñoz et al. 2006). The inferred dark-matter densities of dwarf galaxies suggest a high-redshift collapse for both classical dSphs and UFDs ($z \sim 12$; Strigari et al. 2008), but the dSphs apparently continued to evolve (Orban et al. 2008; Weisz et al. 2011). In contrast, the UFDs are the least chemically-evolved galaxies known, with abundance patterns that imply their star formation was brief (Frebel et al. 2010) and individual stellar metallicities as low as [Fe/H] = –3.7 (Norris et al. 2010). The strict conformance to a metallicity-luminosity relation for all Milky Way satellites limits the amount of tidal stripping to a factor of $\sim$3 in stellar mass (Kirby et al. 2011). Therefore, UFDs are not tidally stripped versions of classical dSphs (see also Penarrubia et al. 2008; Norris et al. 2010).

As one way of solving the missing satellite problem, galaxy formation simulations assume that UFDs formed the bulk of their stars prior to the epoch of reionization (e.g., Tumlinson 2010; Muñoz et al. 2009; Bovill & Ricotti 2009; Koposov et al. 2009). Mechanisms that could drive an early termination of star formation include reionization, gas depletion, and supernova feedback. Using the *Hubble Space Telescope (HST)*, we are undertaking a deep imaging survey of UFDs that reaches the old main sequence (MS) in each galaxy, yielding high-precision color-magnitude diagrams (CMDs) that provide sensitive probes of their star formation histories. The program includes Hercules, Leo IV, Ursa Major I, Bootes I, Coma Berenices, and Canes Venatici II. Here, we give preliminary results for the first three galaxies.

2. OBSERVATIONS AND DATA REDUCTION

We obtained deep optical images of each galaxy (Table 1) using the F606W and F814W filters on the Advanced Camera for Surveys (ACS). These filters efficiently enable a high signal-to-noise ratio (SNR) on the stellar MS and facilitate

[1] Based on observations made with the NASA/ESA *Hubble Space Telescope*, obtained at STScI, which is operated by AURA, Inc., under NASA contract NAS 5-26555.

[2] Space Telescope Science Institute, 3700 San Martin Drive, Baltimore, MD 21218, USA; tbrown@stsci.edu, tumlinson@stsci.edu, jkalirai@stsci.edu, avila@stsci.edu, ferguson@stsci.edu

[3] Astronomy Department, Yale University, New Haven, CT 06520, USA; marla.geha@yale.edu

[4] California Institute of Technology, 1200 East California Boulevard, MC 249-17, Pasadena, CA 91125, USA; enk@astro.caltech.edu

[5] Hubble Fellow

[6] Department of Physics and Astronomy, University of Victoria, P.O. Box 3055, Victoria, BC, V8W 3P6, Canada; vandenbe@uvic.ca

[7] Departamento de Astronomía, Universidad de Chile, Casilla 36-D, Santiago, Chile; rmunoz@das.uchile.cl

[8] Observatories of the Carnegie Institution of Washington, 813 Santa Barbara Street, Pasadena, CA 91101, USA; jsimon@obs.carnegiescience.edu

[9] UCO/Lick Observatory and Department of Astronomy and Astrophysics, University of California, Santa Cruz, CA 95064, USA; raja@ucolick.org

[10] Osservatorio Astronomico, Vicolo Dell'Osservatorio 5, I-35122 Padova, Italy; alvio.renzini@oapd.inaf.it

Table 1
Observations

Name	R.A. (J2000)	Dec. (J2000)	$(m-M)_V$ (mag)	$E(B-V)$ (mag)	M_V (mag)	<[Fe/H]>[a]	[Fe/H] r.m.s.[a]	tiles	Exposure per tile F606W (s)	Exposure per tile F814W (s)	50% complete F606W (mag)	50% complete F814W (mag)
Hercules	16:31:05	+12:47:07	20.90	0.08	–6.2[b]	–2.41	0.6	2	12,880	12,745	29.1	29.1
Leo IV	11:32:57	-00:31:00	21.14	0.07	–5.8[c]	–2.54	0.9	1	20,530	20,530	29.1	29.2
Ursa Major I	10:35:04	+51:56:51	20.10	0.04	–5.5[d]	–2.18	0.7	9	4,215	3,725	28.4	28.4

[a]Kirby et al. (2011), based on Simon & Geha et al. (2007) spectroscopy.
[b]Sand et al. (2009)
[c]de Jong et al. (2010)
[d]Martin et al. (2008)

comparison with other *HST* programs exploring the Local Group. We obtained parallel imaging with the Wide Field Camera 3, but those data are not included here. The image area and depth were chosen to provide a few hundred stars on the upper MS, with a SNR of $\sim$100 near the turnoff. Our image processing includes the latest pixel-based correction (Anderson & Bedin 2010; Anderson 2012, in prep.) for charge-transfer inefficiency (CTI). All images were dithered to mitigate detector artifacts and enable resampling of the point spread function (PSF). We co-added the images for each filter in a given tile using the IRAF DRIZZLE package (Fruchter & Hook 2002), with masks for cosmic rays and hot pixels derived from each image stack, resulting in geometrically-correct images with a plate scale of $0.03''$ pixel^{-1} and an area of approximately $210'' \times 220''$.

We performed both aperture and PSF-fitting photometry using the DAOPHOT-II package (Stetson 1987), assuming a spatially-variable PSF constructed from isolated stars. The final catalog combined aperture photometry for stars with photometric errors $<$0.02 mag and PSF-fitting photometry for the rest, all normalized to an infinite aperture. Due to the scarcity of bright stars, the uncertainty in the normalization is $\sim$0.02 mag. Our photometry is in the STMAG system: $m = -2.5\times \log_{10} f_\lambda - 21.1$. For galaxies with multiple tiles, the ridge line in each tile was compared to that in other tiles; we then made small ($\sim$0.01 mag) color adjustments to force agreement between tiles, ensuring the full catalog for a galaxy did not have larger photometric scatter than that in any tile. The catalogs were cleaned of background galaxies and stars with poor photometry, rejecting outliers in χ^2 (from PSF fitting), PSF sharpness, and photometric error. We also rejected stars with bright neighbors or falling within extended background galaxies. We performed artificial star tests to evaluate photometric scatter and completeness, including CTI effects, with the same photometric routines used to create the actual photometric catalogs.

The CMD of each UFD galaxy is shown in Figure 1. Each UFD is clearly dominated by an ancient population. Field contamination is significant, but is particularly high in the vicinity of the red giant branch (RGB), increasing its apparent breadth. In Hercules and Leo IV, the star counts are a bit lower than expectations from ground surveys (Muñoz et al. in prep.), while the counts in Ursa Major I are significantly lower, but the sample is large enough to judge its population relative to those of the other two galaxies.

3. ANALYSIS

3.1. *Comparison to M92*

As one of the most ancient, metal-poor, and well-studied globular clusters, M92 is an important empirical fiducial for the UFD galaxies. It was previously observed by Brown et al. (2005) with ACS, using the same filters employed here, as one of six empirical templates for deep CMD analyses of Andromeda (e.g., Brown et al. 2006). Since then, estimates of the M92 distance modulus have generally drifted $\sim$0.1 mag higher, and estimates for the metallicity have generally decreased by $\sim$0.2 dex. Here, we assume values that are representative of the current literature (Del Principe et al. 2005; Sollima et al. 2006; Paust et al. 2007; VandenBerg et al. 2010; Benedict et al. 2011), with $(m-M)_V$ = 14.69 mag, $E(B-V)$ = 0.023 mag, and [Fe/H] = –2.3. Because the UFD metallicity distribution extends much lower than that of any globular cluster, the age determination must rely upon theoretical isochrones (see §3.2), but a comparison to M92 is still instructive.

In our analysis, the largest uncertainties are the distances of the UFDs relative to the globular clusters used to calibrate our isochrone library, with emphasis on M92. For each UFD, we started with recent literature values, then made small adjustments to the distance and reddening, such that placing the M92 fiducial in the UFD frame would produce acceptable alignments at the horizontal branch (HB), RGB, and the MS, with the alignments at the RGB and MS accounting for the metallicity distribution and a reasonable binary fraction. Spectroscopy of RGB stars in these UFDs finds a broad range of metallicity ($-3.2 \lesssim$ [Fe/H] $\lesssim -1$), with the bulk of the stars having [Fe/H]< -2 (Simon & Geha 2007; Kirby et al. 2008). Although the binary fraction is largely unconstrained in the UFDs, we assume a binary fraction of 30%, matching that in the globular cluster Palomar 13 (Clark et al. 2004), given that the blue straggler population in the UFDs is similar to that in Palomar 13 (Bradford et al. 2011).

In Table 1, we show our assumed apparent distance moduli, which are somewhat larger than previous literature measurements, in part because our assumed reddening values are 0.02–0.03 mag larger than the values of Schlegel et al. (1998) along these sightlines. For Hercules, we find $(m-M)_V$ = 20.90 mag, compared to Sand et al. (2009), who found $(m-M)_V = 20.7\pm0.1$ mag. For Leo IV, we find $(m-M)_V$ = 21.14 mag, compared to Moretti et al. (2009), who found $(m-M)_V = 21.06\pm0.08$ mag using RR Lyrae stars in the galaxy (associated with an old population). For Ursa Major I, we find $(m-M)_V$ = 20.10 mag, compared to Okamoto et al. (2008), who found $(m-M)_V = 19.99\pm0.1$ mag. Note that if we were to assume the shorter distance moduli in the literature, the UFD ages relative to M92 would increase. The UFD CMDs would not change (they reflect the observed distribution of color and magnitude), but the M92 ridge line would shift brighter due to the shorter assumed distance for the UFD, making the MS turnoff in each galaxy appear fainter (and thus older) relative to that in M92, which would significantly vio-

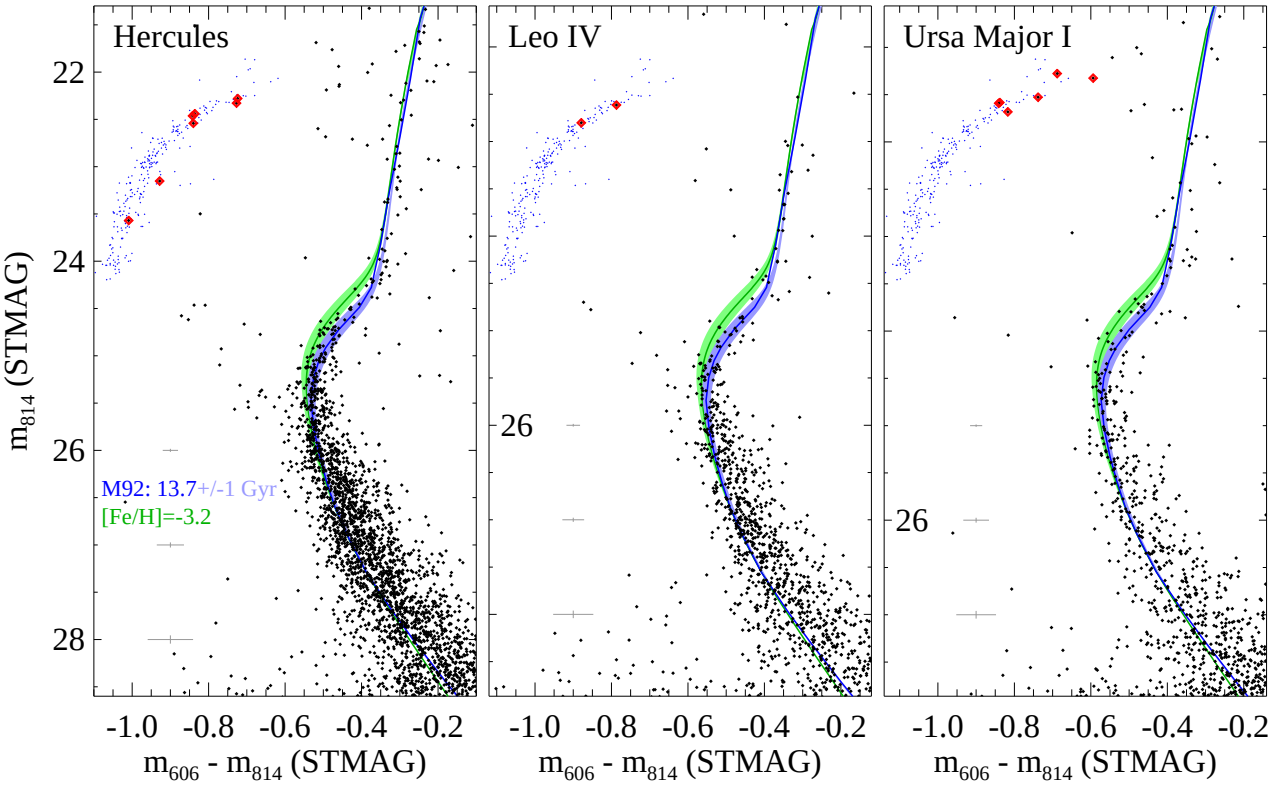

Figure 1. The CMD of each UFD (black points), with axes shifted to ease comparisons. For reference, we show the empirical ridge line for the MS, SGB, and RGB in M92 (dark blue curve), along with the HB locus in M92 (blue points). The M92 fiducial has been placed at the distance and reddening for each galaxy, matching the luminosity of HB stars in each UFD (highlighted in red) and the color of the RGB and MS stars in each UFD (accounting for the metallicity distribution and a reasonable binary fraction of 30%). The light blue band is bounded by isochrones within 1 Gyr of M92's age (13.7 Gyr), at the M92 metallicity ([Fe/H]=−2.3), showing excellent agreement with the M92 ridge line. Because the UFD metallicities extend much lower than those in globular clusters, we also show an isochrone at the age of M92 but at the low extreme of the metallicity distribution ([Fe/H]=−3.2; dark green curve), bounded by isochrones offset by 1 Gyr (light green band). A blue straggler sequence is present in each galaxy, but there are no stars significantly younger than M92.

late the age of the universe (13.75 ± 0.11; Jarosik et al. 2011) unless other factors (e.g., CNO abundances) were adjusted accordingly.

With these caveats, we show the comparison of each UFD to M92 in Figure 1. Although there are only a few HB stars in each UFD (red points), their luminosities agree with those of the HB stars in M92 (blue points) for our assumed distance and reddening. HB morphology is most sensitive to metallicity (but also age and the abundances of He and CNO), with the HB color distribution shifting toward the blue at lower [Fe/H]. The colors of the HB stars in each UFD are consistent with their metallicities, in the sense that <[Fe/H]> is slightly higher in Ursa Major I than in Hercules or Leo IV (Table 1), and its HB stars are somewhat redder, but this may be due to small number statistics. The width of the RGB appears slightly wider than one would expect from the photometric errors and metallicity distribution, but this is uncertain, given the field contamination. The MS turnoff and subgiant branch (SGB) in each UFD extends slightly brighter and bluer than those features on the M92 ridge line. If we did not know the metallicity distributions, we would conclude that the brighter and bluer stars have ages a few Gyr younger or metallicities up to ∼1 dex lower than M92. However, we know the UFD metallicities extend below [Fe/H] = −3, so these stars are consistent in age with M92, as we show below.

3.2. *Comparison to Theoretical Isochrones*

Because the UFDs are among the most metal-poor populations in the local universe, we cannot rely solely upon empirical stellar population templates (e.g., globular clusters) to analyze them. We must extend these empirical templates to lower metallicities using theoretical models. For this purpose, we employ the Victoria-Regina isochrones (VandenBerg et al. 2010, 2012).

Compared to the previous version of the code (VandenBerg et al. 2006), the current version includes, among other things, the effects of He diffusion, the latest improvements to the H-burning nuclear reaction rates, and an update to the Asplund et al. (2009) solar metals mixture. The net effect of these changes is to reduce the age at a given turnoff luminosity by ∼0.5 Gyr. Our purpose here is to use these isochrones to derives ages *relative* to those of the globular clusters, but any comparisons to other work in the literature should keep in mind these effects when considering absolute ages.

Brown et al. (2005) produced a set of empirical population templates in the ACS F606W and F814W filters, spanning a wide metallicity range, based upon Galactic globular and old open clusters. They then calibrated a transformation of the Victoria-Regina isochrones into the same filters, producing agreement at the ∼1% level. Here, we have adjusted this transformation at the level of ∼0.03 mag in color. This adjustment accounts for the new version of the Victoria-Regina isochrones and the current state of the literature regarding cluster parameters. These isochrones match the ACS CMDs of 47 Tuc at an age of 12.3 Gyr, NGC 6752 at an age of 13.2 Gyr, and M92 at an age of 13.7 Gyr. As discussed in §3.1, M92 is the most relevant calibrator, but the other clusters demonstrate that the isochrones are valid over a wide range of

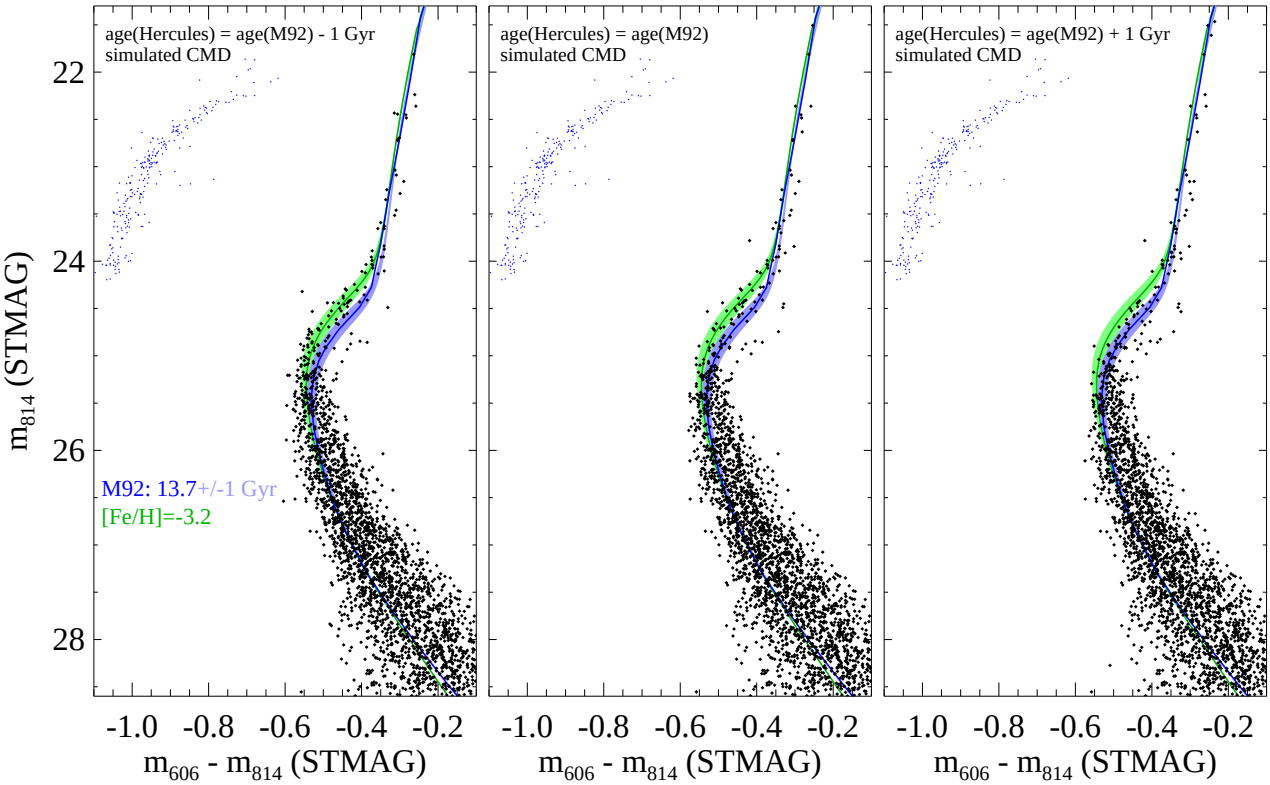

Figure 2. Simulated CMDs for Hercules (MS–RGB) under three assumptions: a population 1 Gyr younger than M92 (left panel), a population at the age of M92 (middle panel), and a population 1 Gyr older than M92 (right panel). To ease comparison with the observed Hercules CMD, these simulations are plotted on the same scale as Figure 1 and include the same empirical and theoretical fiducials (colored curves). The middle panel best matches the observed Hercules CMD, given the luminosity distribution of the SGB stars and the color of the MS turnoff (bluest point on the MS).

[Fe/H] (–0.7 to –2.3). We stress that these absolute ages depend critically upon the assumed distance moduli and oxygen abundances.

In Figure 1, we show the expected location of stars in the ACS CMDs for ages within a Gyr of the M92 age (i.e., 12.7–14.7 Gyr) at two different metallicities: that of M92 (i.e., [Fe/H]= –2.3; blue curve) and the low extreme of the metallicity distribution in these UFDs ([Fe/H]= –3.2; green curve). It is clear from the comparison that the luminosity of the MS turnoff and SGB in each galaxy is consistent with extremely ancient metal-poor stars. The few stars immediately brighter and bluer than the old MS turnoff are blue stragglers, which are ubiquitous in old populations. If these were young stars, each UFD would have a star-formation history consisting of two delta functions in age, with a few percent of the stars at ∼4 Gyr and the rest at 13.7 Gyr; continuous low-level star formation would produce intermediate-age MS and SGB stars that are not observed.

Although the MS turnoff becomes bluer and brighter at both younger ages and lower metallicities, this age-metallicity degeneracy can be broken by simultaneously fitting the MS, SGB, and RGB in a CMD. However, the scarcity of RGB stars and multitude of field stars precludes this type of fit here. Instead, we rely upon the observed metallicity distribution from spectral synthesis of neutral Fe lines (Kirby et al. 2008; based upon Keck spectroscopy from Simon & Geha 2007). For the current analysis, we will use the relatively well-populated CMD of Hercules as an example, employing the 15 RGB stars with low spectroscopic errors (<0.3 dex) observed to date. We use the artificial star tests from Hercules to produce a library of simple stellar populations spanning $-1.4 > [Fe/H] > -3.2$ and ages of 10–16 Gyr that have the same photometric properties (scatter and completeness) as the observed Hercules CMD. We then perform a Maximum Likelihood fit to that part of the Hercules CMD where the age leverage is greatest ($24.0 < m_{F814W} < 25.7$ mag), varying the age distribution while holding the metallicity fixed. We find a mean age of 13.7 Gyr for Hercules (i.e., the same age as M92). Formally, the statistical uncertainty is ∼0.2 Gyr, but the systematic uncertainties (e.g., assumed distance and oxygen abundance) are much larger (∼1 Gyr).

We show in Figure 2 three simulated CMDs for Hercules, using the above library of scattered isochrones. Each CMD assumes the observed spectroscopic metallicity distribution for Hercules, under three age assumptions: 1 Gyr younger than M92 (left panel), the same age as M92 (middle panel), and 1 Gyr older than M92 (right panel). We assume a Salpeter initial mass function (IMF), which appears to be a reasonable assumption; we note that our photometry provides interesting IMF constraints over the mass range ∼0.5–0.9 $M_{\odot}$ (Geha et al. in prep.). It is clear that the best match to the observed Hercules CMD (Figure 1) is the middle panel, where the populations have the same age as M92. Although the population statistics are best in Hercules, the similarity of the Leo IV and Ursa Major I CMDs implies that they also host populations of approximately the same age. None of these galaxies appears to host a significant population of stars younger than M92 (13.7 Gyr).

In the Hercules spectroscopy, approximately 20% of the RGB stars fall at $[Fe/H] = -1.7 \pm 0.3$. In the Hercules CMD (Figure 1), the stars immediately below the M92 SGB, especially near the MS, are consistent with such stars at ages

within a Gyr of M92 (cf. Figure 2), although the exact number is uncertain, given the field contamination. However, if any of these stars at [Fe/H]> -2 were as much as 2 Gyr younger than M92, they would be difficult to discern in the Hercules CMD, because the SGB for such stars would fall within the dominant SGB observed for Hercules (i.e., within the region bounded by the blue and green fiducials of Figure 1). Thus, while it is clear that most stars in Hercules are as old as those in M92, we cannot at this time rule out a minority sub-population of stars (up to $\sim$10% of the total population) that are 1–2 Gyr younger at the high end of the Hercules metallicity distribution.

4. DISCUSSION

The three UFD galaxies here are among the more distant of those known in the Milky Way system, at 100–150 kpc, so ground-based CMDs of each implied they were old ($>$10 Gyr), but could not put tight constraints on their ages (e.g., Sand et al. 2009; Sand et al. 2010; Okamoto et al. 2008, 2012). Our *HST* observations reach well below the MS turnoff in each galaxy, revealing that all three host truly ancient metal-poor populations. The majority of the stars in each galaxy must have ages within 1 Gyr of M92's age, with younger ages strongly ruled out, although we cannot exclude a trace population of stars 1–2 Gyr younger than M92 at the high end of the metallicity distribution.

Two UFD galaxies (Bootes I and Coma Berenices) are significantly closer (44–66 kpc), such that ground-based CMDs can place constraints on their ages approaching what can be done with *HST* (Muñoz et al. 2010; Okamoto et al. 2012). These CMDs also imply ages approximately as old as M92, although the use of distinct bandpasses hampers accurate comparisons to our observations. Our *HST* survey includes these galaxies, enabling accurate age measurements in a significant sample of UFDs, with all observed in the same photometric system as each other and the most ancient globular clusters.

If we include Bootes I and Coma Berenices, it seems likely that at least 5 UFD galaxies have ages consistent with that of the oldest known globular cluster (M92), with no evidence for significantly younger populations. This is in striking contrast to any other galaxy class in the local universe. Our external vantage point for Andromeda enables accurate ages throughout its halo, using the same instrument and techniques described here, yet all such measurements to date have found an extended star formation history, with significant numbers of stars younger than 10 Gyr (Brown et al. 2006, 2008). An *HST* survey of 60 dwarf galaxies within 4 Mpc found that most formed the bulk of their stars prior to $z \sim 1$, but none were consistent with a purely ancient population (Weisz et al. 2011). The UFDs may be the only galaxies where star formation ended in the earliest epoch of the universe. If so, the apparent synchronicity to their star formation histories suggests a truncation induced by a global event, such as reionization (13.3 Gyr ago; Jarosik et al. 2011). The UFDs were likely the victims of reionization, rather than the agents, given the small numbers of stars available to produce ionizing photons.

Support for GO-12549 was provided by NASA through a grant from STScI, which is operated by AURA, Inc., under NASA contract NAS 5-26555. ENK acknowledges support by NASA through Hubble Fellowship grant 51256.01 from STScI. AR acknowledges support from ASI via grant I/009/10/0. R.R.M. acknowledges support from the GEMINI-CONICYT Fund, allocated to the project N°32080010.

REFERENCES

Anderson, J., & Bedin, L.R. 2010, PASP, 122, 1035
Asplund, M., Grevesse, N., Sauval, A.J., & Scott, P. 2009, ARAA, 47, 481
Baumgardt, H., Côté, P., Hilker, M. Rejkuba, M., Mieske, S., Djorgovski, S.G., & Stetson, P. 2009, MNRAS, 396, 2051
Belokurov, V., et al. 2007, ApJ, 654, 897
Benedict, G.F., et al. 2011, AJ, 142, 187
Bovill, M.S., & Ricotti, M. 2009, ApJ, 693, 1859
Bradford, J.D., et al. 2011, ApJ, 743, 167
Brown, T.M., et al. 2005, AJ, 130, 1693
Brown, T.M., et al. 2006, ApJ, 323, 353
Brown, T.M., et al. 2008, ApJ, 685, L121
Clark, L.L., Sandquist, E.L., & Bolte, M. 2004, AJ, 128, 3019
de Jong, J.T.A., Martin, N.F., Rix, H.-W., Smith, K.W., Jin, S., & Macció, A.V. 2010, ApJ, 710, 1664
Del Principe, M., Piersimoni, A.M., Bono, G., Di Paola, A., Dolci, M., Marconi, M. 2005, AJ, 129, 2714
Frebel, A., Simon, J.D., Geha, M., & Willman, B. 2010, ApJ, 708, 560
Fruchter, A.S., & Hook, R.N. 2002, PASP, 114, 144
Jarosik, N., et al. 2011, ApJS, 192, 14
Kalirai, J.S., et al. 2010, ApJ, 711, 671
Kirby, E.N., Simon, J.D., Geha, M., Guhathakurta, P., & Frebel, A. 2008, ApJ, 685, L43
Kirby, E.N., Lanfranchi, G.A., Simon, J.D., Cohen, J.G., & Guhathakurta, P. 2011, ApJ, 727, 78
Kleyna, J.T., Wilkinson, M.I., Wyn Evans, N., & Gilmore, G. 2005, ApJ, 630, L141
Koposov, S.E., Yoo, J., Rix, H.-W., Weinberg, D.H., Macció, A.V., & Escudé, J.M. 2009, 696, 2179
Martin, N.F., de Jong, J.T.A., & Rix, H.-W. 2008, ApJ, 684, 1075
McConnachie, A.W., et al. 2009, Nature, 461, 66
Moore, B., Ghigna, S., Governato, F., Lake, G., Quinn, T., Stadel, J., & Tozzi, P. 1999, ApJ, 524, L19
Moretti, M.I., et al. 2009, AJ, 699, L125
Muñoz, J.A., Madau, P., Loeb, A., & Diemand, J. 2009, MNRAS, 400, 1593
Muñoz, R.R., Carlin, J.L., Frichaboy, P.M., Nidever, D.L., Majewski, S.R., & Patterson, R.J. 2006, ApJ, 650, L51
Muñoz, R.R., Geha, M., & Willman, B. 2010, AJ, 140, 138
Norris, J.E., et al. 2010, ApJ, 723, 1632
Orban, C., Gnedin, O.Y., Weisz, D.R., Skillman, E.D., Dolphin, A.E., & Holtzman, J.A. 2008, ApJ, 686, 1030
Okamoto, S., Arimoto, N., Yamada, Y., & Onodera, M. 2008, A&A, 487, 103
Okamoto, S., Arimoto, N., Yamada, Y., & Onodera, M. 2012, ApJ, 744, 96
Paust, N.E.Q., Chaboyer, B., & Sarajedini, A.. 2007, AJ, 133, 2787
Peñarrubia, J., et al. 2008, ApJ, 673, 226
Sand, D.J., et al. 2009, ApJ, 704, 898
Sand, D.J., et al. 2010, ApJ, 718, 530
Schlegel, D.J., Finkbeiner, D.P., & Davis, M. 1998, ApJ, 500, 525
Simon, J.D., & Geha, M. 2007, ApJ, 670, 313
Sollima, A., Cacciari, C., & Valenti, E. 2006, MNRAS, 372, 1675.
Stetson, P.B. 1987, 99, 191
Strigari, L.E., Bullock, J.S., Kaplinghat, M., Simon, J.D., Geha, M., Willman, B., & Walker, M.G. 2008, Nature, 454, 1096
Tumlinson, J. 2010, ApJ, 708, 1398
van de Ven, G., van den Bosch, R.C.E., Verolme, E.K., & de Zeeuw, P.T. 2006, A&A, 445, 513
VandenBerg, D.A., Bergbusch, P.A., Dotter, A., Ferguson, J., Michaud, G., & Proffitt, C.R. 2012, ApJ, submitted
VandenBerg, D.A., Bergbusch, P.A., & Dowler, P.D. 2006, ApJS, 162, 375
VandenBerg, D.A., Casagrande, L., & Stetson, P.B. 2010, AJ, 140, 1020
Weisz, D.R., et al. 2011, ApJ, 739, 5
Willman, B., et al. 2005, AJ, 129, 2692
York, D.G., et al. 2000, AJ, 120, 1579
Zucker, D.B., et al. 2006, ApJ, 650, L41
Zucker, D.B., et al. 2007, ApJ, 659, L21